# Correlation between microvoid properties and mechanical properties of polyoxymethylene strained beyond yield

**J. H. Wendorff**
*Deutsches Kunststoff-Institut, 6100 Darmstadt, West Germany*
*(Received 14 June 1979; revised 18 October 1979)*

The shape, size distribution and concentration of microvoids were determined as a function of the strain for strained polyoxymethylene. Using a specific molecular model for the mechanism of microvoid formation, it became possible to calculate the energetic content of the microvoids. This energy was found to be directly related to a component of the mechanical energy, which was absorbed during a stress–strain experiment. The relation between the shape of the stress–strain curve of polyoxymethylene and the mechanism of microvoid formation is discussed.

## INTRODUCTION

Fracture of polymers is influenced strongly by the existence of stress raising flaws[1,2]. Inhomogenities (e.g. surface scratches, internal voids, interfaces between different components and phases of the material) or irregularities on a molecular scale (e.g. dislocations in crystals) lead to local stresses which may exceed the nominal stress by several orders of magnitude. The stress concentration is related to the particular geometry of the flaws. According to theory, fracture occurs if the flaws become capable of propagating.

It is less well known that, in many cases, flaws initiated in stressed materials do not cause fracture as long as they are not able to propagate, but nevertheless influence macroscopical properties to a great extent. Macroscopical properties such as stress–strain behaviour may be correlated with energetic and geometric properties of particular flaws.

These properties of flaws can be studied in principal by a variety of techniques. The choice of the particular method depends on the nature and size of the flaws to be analysed. Indirect methods for analysing flaw formation were devised by Retting[3]. Acoustic emission studies yield only general information on flaw formation[4,5]. Optical methods and electron microscopy were used in order to detect crazes in amorphous and partially crystalline polymers[6–8]. Flaw formation due to chain scission was analysed by means of e.s.r. spectroscopy[9–11,21,22]. Small angle X-ray diffraction has been used for a variety of amorphous and partially crystalline polymers to characterize crazes and, in particular, microvoids. Microvoids are initiated in many polymers which are subjected to mechanical stresses[12–18,21,22]. It has to be pointed out, however, that different mechanisms of microvoid formation occur in polymers[17,18]. The specific kind observed depends on the mode of deformation – homogenous or inhomogeneous deformation via neck formation, continuous or cyclic deformation – and on the structure of the polymers – amorphous or partially crystalline material. These details require more attention in the future.

One of the polymers studied by our employing the method of small angle X-ray scattering was polyoxymethylene[17,18]. We found that both static and dynamic stresses resulted in the formation of microvoids. It is the aim of this paper to relate macroscopical mechanical properties to the properties of the defects and to analyse the process by which the defects influence macroscopical properties.

### *Properties of microvoids*

We were able to show in earlier papers[17,18] that microvoids are created in polyoxymethylene samples, if these are subjected to static or dynamic tensional stresses. In the case of a continuous homogeneous deformation, we found that the average shape of these microvoids approximates to a rotational ellipsoid with diameters between 9 and 20 nm. The small axis of the ellipsoid – the axis of rotation – coincides with the draw direction.

The distribution of the size and the shape of the microvoids can be represented by an exponential density correlation function $C(r)$:

$$C(r) = \langle(\delta\eta(x)\delta\eta(x+r))/\delta\eta(x)^2\rangle = \exp(-r/a) \qquad (1)$$

$x$ and $(x + r)$ are two locations separated by a distance $r$ within the sample containing microholes. $\delta\eta(x)$ represents the electron density difference between the microvoid and the polymer matrix. The average size of the microvoid $d$ is related to the correlation length $a$ by[19]:

$$d = a/(1 - v) \qquad (2)$$

where $v$ is the volume fraction of microvoids. Thus $d$ is given approximately by the value of the correlation length $a$ for small values of $v$.

The value of the correlation length in a particular direction within the stressed sample is independent of the strain, whereas the number of microvoids increased exponentially with increasing strain.

The microvoids are not able to relax at room temperature

0032–3861/80/050553–06$02.00

in the stress-free state; however, they vanish at increased temperatures. This behaviour will be analysed in detail since it can be used to reconstruct the shape and size distribution of the microvoids in the stressed material.

The size of the microvoids increased simultaneously in all directions under the influence of an external unidirectional load. The deformation was characterized by a creep compliance of the microvoids which was much larger than the corresponding value of the macroscopic sample.

By analysing the creep and relaxation behaviour of the microvoids, we concluded that microvoids are initiated by translational motions of single crystalline regions (mosaic blocks) of the lamellae in the drawing direction in this particular case. The microvoids occur in amorphous regions between the lamellae. Although these regions should have a low viscosity – the glass transition temperature is below room temperature – they are not able to exhibit the properties of ideal fluids, since the chain molecules in these regions are attached to the neighbouring crystalline regions. This results in a hindered viscous flow: the amount of possible translational displacements is limited.

We have proposed a mechanical model which accounts for the observed behaviour. It consists of an ideal fluid contained in a hollow cylinder with two pistons at its ends. A void located in the fluid will increase its size simultaneously in all directions, if the volume of the system is increased due to the motion of the pistons. This motion represents the translational motion of the mosaic blocks in stressed samples.

According to this model, the stress $\sigma_D$ acting on the piston due to the voids is proportional to the surface free energy $\sigma_l$ of the fluid and inversely proportional to the average diameter $d$ of the voids:

$$\sigma_D = A\sigma_l/d \tag{3}$$

where $A$ is a geometric factor which depends on the shape of the void. In the case of a spherical shape, $A$ equals 4. This model will be used below in order to calculate energetic properties of microvoids. The surface free energy $\sigma_l$ may contain contributions from plastic flow components, orientation effects and chain breakages in this general description, as in the case of crack formation and propagation[1,21]. According to our model, however, these contributions should be small in the case considered here. The absolute value of the surface free energy will be discussed below with respect to this problem.

## EXPERIMENTAL

### *Samples*

Molten samples of polyoxymethylene (Hostaform T 1020, a copolymer from Hoechst AG, West Germany) were crystallized from the melt at a crystallization temperature of 155°C (sample A) or quenched from the melt in cold water (sample B). The degree of crystallinity, as determined by differential scanning calorimetry (d.s.c.) and wide angle X-ray diffraction, was about 0.75 for sample A and 0.63 for sample B. Their melting temperatures were 170° and 168°C respectively.

### *Stress–strain experiments*

Stress–strain curves were determined for both kinds of samples using a constant deformation rate of $\dot{\epsilon} = 0.1\ \text{min}^{-1}$. Each particular experiment consisted of straining the sample up to a definite strain $\epsilon_f$ after which the stress was removed immediately. Subsequently, the sample was allowed to relax at room temperature for about 400 h. The stress–strain experiments were then repeated, taking the same value of $\dot{\epsilon}$ and $\epsilon_f$ as in the first run. The whole procedure was repeated several times for each sample. $\epsilon_f$ was varied between 0.02 and 0.16.

### *Small angle X-ray scattering*

A Kratky small angle X-ray camera was employed. The excess scattering $\Delta I$, which is the difference between the scattering curve of the strained and the unstrained sample, was analysed in terms of particle scattering, since it was found to decrease continuously with increasing scattering vector $\vec{s}$ ($|\vec{s}| = s = 4\pi\sin\theta/\lambda$, $2\theta$ is the scattering angle, $\lambda$ the wave length of radiation). The scattering could be described on the basis of the electron density correlation function $C(r)$ discussed above (equation (1))[19]. It gives rise to the following smeared scattering curve $\Delta I$ which is experimentally obtained if a Kratky camera is used:

$$\widetilde{\Delta I}(s) = I_e V\langle\delta\eta(x)^2\rangle 4\pi a^2/(1 + a^2s^2)^{3/2} \tag{4}$$

where $I_e$ is the scattering by an electron and $V$ the scattering volume. The correlation length $a$, characterizing the average diameter of the particles, can thus be obtained from the slope and the intercept of a plot of $\widetilde{\Delta I}^{-2/3}$ *versus* $s^2$ which should yield a straight line.

The concentration of the microvoids can be calculated[20] from the value of the invariant $I_n$, if we assume that the electron density of the microvoids is approximately zero:

$$I_n = \int \widetilde{\Delta I}(s)s\,ds \approx 4\pi^2 I_e V\eta_M^2 \nu(1-\nu) \tag{5}$$

where $\eta_M$ is the electron density of the polymer matrix. Absolute scattering intensities, which are necessary in order to calculate the concentration of microvoids in the samples, were obtained by comparing the excess scattering with the scattering of a calibration sample which was kindly provided by Prof. Kratky.

Since the correlation length depended in our case on the direction within the sample, we determined the invariant $I_n$ using a geometry in which the slitwise primary beam was parallel to an axis of orientation. This axis coincided with th draw direction.

## RESULTS

### *Stress–strain experiments*

The stress–strain curves of previously unstrained samples were characterized by an almost linear increase of the stress with increasing strain up to a strain of about 0.01 (*Figure 1*). The stress became independent of the strain if the strain exceeded 0.06. The yielding took place without neck formation, at least on a macroscopical scale. The yield stress $\sigma_a$ of sample A, crystallized from the melt at 155°C was slightly larger than the corresponding value of sample B. The values were 65 N mm$^{-2}$ and 55 N mm$^{-2}$, respectively, at room temperature.

Hysteresis effects, which were observed for both kinds of samples, indicated that, within the time scale studied here, an appreciable part of the total deformation energy was not released on removal of the stress. The residual strain of the previously strained sample was found to be small in

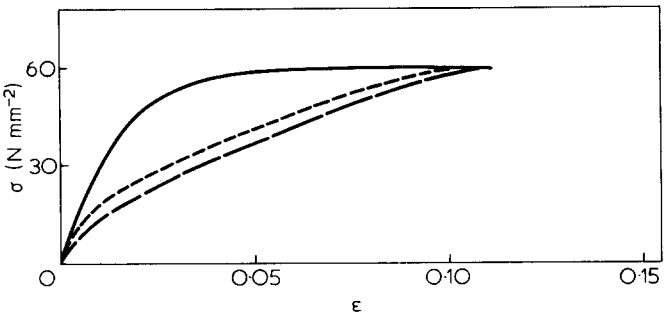


*Figure 1* Stress–strain curves of polyoxymethylene, sample A, $\epsilon_f = 0.12$. First run, (——); second run, (— — —); third run, (—— ——)

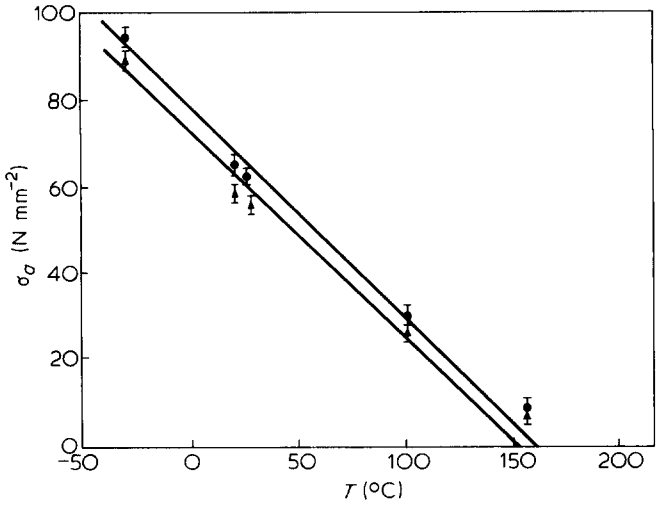


*Figure 2* Dependence of yield stress $\sigma_a$ of polyoxymethylene on temperature $T$. Sample A, ●; sample B, ▲

comparison to the strain $\epsilon_f$. Most of it vanished if the samples were allowed to relax in the stress-free state for 400 h at room temperature.

The yield stress $\sigma_a$ decreased approximately with increasing temperature for both kinds of samples in the temperature range between −30°C and 155°C. This behaviour may be roughly represented by a linear relation:

$$\sigma_a = \sigma_{ao} - jT \qquad (6)$$

$\sigma_{ao}$ and $j$ are constants, as shown in *Figure 2*.

Large deviations occurred between the original stress–strain curves and the stress–strain curves of previously strained samples, even if these had been allowed to relax for 400 h (*Figure 1*). These deviations increased with increasing final strain $\epsilon_f$ (*Figure 3*). The energy necessary to obtain a specific strain was lowered due to a previous strain for strains $\epsilon_f$ exceeding 0.03. This result showed that energy was apparently absorbed by the sample during the first deformation process; this was not totally dissipated to heat, but was stored in the material and remained there despite relaxation processes which had taken place. The energy storage will be treated below in more detail.

The dependence of the energy stored in the samples $G_M$ on the strain can be represented by the following expression:

$$G_M(\epsilon_f) = A + B\exp(\epsilon_f) \qquad (7)$$

since a plot of $\ln G_M$ *versus* $\epsilon_f$ yields a straight line, as shown in *Figure 4*. $A$ and $B$ are constants.

The value of $G_M(\epsilon_f)$ increased with an increasing number of deformation runs. The incremental increase per run is much larger in the first run as compared to the following runs (see *Figure 1*).

The differences between the stress strain curves of the unstrained and the previously strained samples decreased strongly, if the strained samples were annealed at temperatures in the range between about 40° and 155°C. The mechanically stored energy is thus partially recoverable. This behaviour will be described in detail in a subsequent paper.

*Defect properties*

The size distribution of the microvoids in strained samples can be evaluated on the basis of experimental data of their annealing behaviour, as already mentioned.

It was observed that the defect concentration decreased within several minutes, if the samples were heated up to a specific annealing temperature $T_a$, and became constant after this time. This process is irreversible; the defect concentration could not be increased again by cooling down to room temperature. *Figure 5* shows the inverse dependence of the defect concentration on the annealing temperature $T_a$. This result indicated that only specific microvoids are able to relax at each particular annealing temperature.

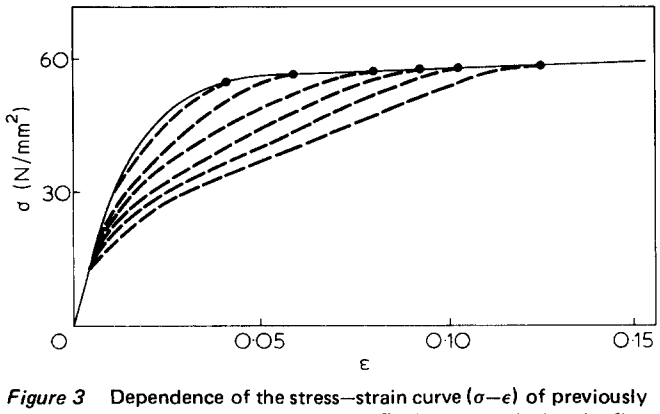


*Figure 3* Dependence of the stress–strain curve ($\sigma$–$\epsilon$) of previously strained polyoxymethylene samples on final strain $\epsilon_f$ during the first run. First run, ——; second run, — — —; $\epsilon_f$ during the first run, ●

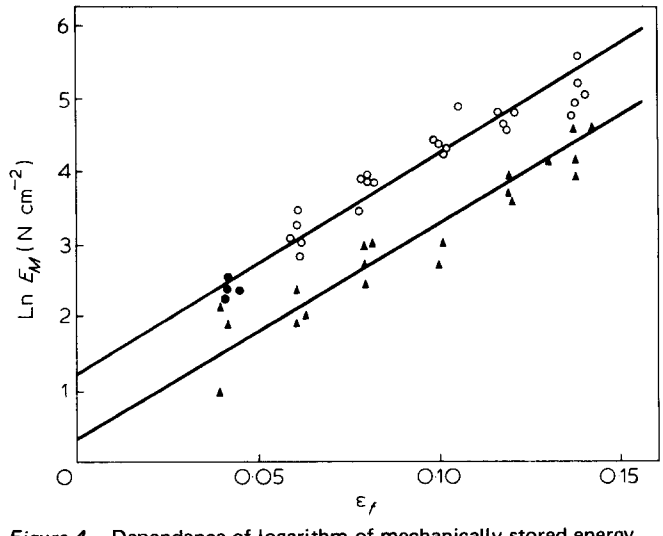


*Figure 4* Dependence of logarithm of mechanically stored energy $G_M$ on strain $\epsilon_f$. Sample A, ●, ○; sample B, ▲

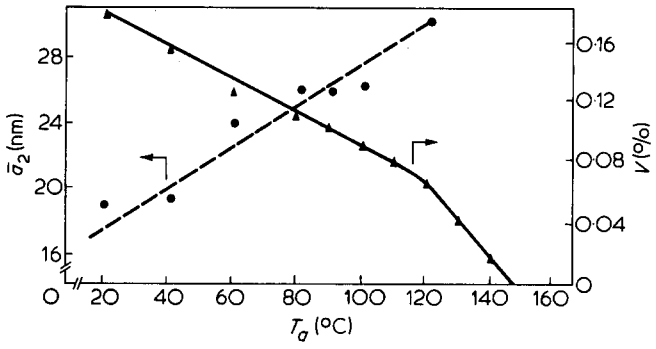


*Figure 5* Dependence of residual defect concentration $\nu$ and correlation length $\bar{a}_2$ (perpendicular to strain direction) on annealing temperature $T_a$

Information on the specific parameters which determine this behaviour are obtained by analysing the dependence of the average sizes of the microvoids on the annealing temperature, both in the direction of the stress and perpendicular to it. These values increase continuously and irreversibly with increasing $T_a$, as shown in *Figure 5*. The result shows that smaller microvoids out of the total distribution relax at low annealing temperatures whereas larger microvoids are still stable at this temperature. This leads to a shift of the average size of the microvoids. The process continues up to temperatures close to the melting point of the material, where only a minor fraction of the original size distribution of the microvoids still exists, characterized by large values of the correlation length. The original distribution is thus continuously depleted with increasing $T_a$.

This result offers the possibility to reconstruct the distribution of microvoids in the strained samples. Let us consider the size distribution of particles – microvoids in the case considered here – which is assumed to be represented by a discrete number $(i-1)$ of components. Each component is characterized by the three diameters $a_{k,i-1}$ $(k = 1, 2, 3)$ of the particles in a specific coordinate system and by their number $N_{i-1}$. The average diameter is given by:

$$\bar{a}_{k,i-1} = \sum_{j=1}^{i-1} N_j a_{k,j} \Big/ \sum_{j=1}^{i-1} N_j \tag{8}$$

This value is obtainable from the scattering curve (equation 4). The average volume of the particles is given by:

$$\bar{V}_{i-1} = V_{total,i-1} \Big/ \sum_{j=1}^{i-1} N_j \tag{9}$$

This value can be calculated from the value of the invariant $I_n$ (equation (5)), provided that the total number of particles is known.

Since we consider microvoids with the shape of rotational ellipsoids and the diameters in particular directions can fluctuate independently from each other, due to the specific mode of microvoid formation, we can represent the value of the average volume of the microvoids by:

$$\bar{V}_{i-1} = 4\pi/3 \sum_{j=1}^{i-1} N_j (a_{1,j}/2)(a_{2,j}/2)^2 \Big/ \sum_{j=1}^{i-1} N_j$$

$$= \pi/6\, \bar{a}_{1,i-1} \bar{a}^2_{2,i-1} \tag{10}$$

This value can be determined thus from the scattering curves.

If an additional component, characterized by the parameters $a_{k,i}$ and $N_i$ is added to the original distribution, we get a new distribution characterized by the average value $\bar{a}_{k,i}$, $\bar{V}_i$ and $V_{total,i}$. These experimentally obtainable values can then be used to calculate the characteristic parameters of the component $i$. Starting from equations (8)–(10) we obtain:

$$N_i = \left( V_{total,i} - \sum_{j=1}^{i-1} N_j \bar{V}_j \right) \Big/ \bar{V}_i \tag{11}$$

$$a_{k,i} = \left( \sum_{j=1}^{i-1} N_j + N_i \right) \bar{a}_{k,i} - \sum_{j=1}^{i-1} N_j a_{k,j} \Big/ N_i \tag{12}$$

If we now assume that at a temperature close to the melting point only one component still exists, that is if we allow:

$$\bar{a}_{k,1} = a_{k,1} \tag{13}$$

we are able to reconstruct the original distribution on the basis of the equations (11) and (12) step-by-step, using the data obtained from the annealing experiment. Equation (13) does not seriously influence the distribution obtained by this procedure due to the small number of particles of the component 1. The distribution $N(a_K)$ shown in *Figure 6* can be represented by an exponential expression, since a plot of $\ln N(a_k)$ *versus* $a_k$ yields straight lines both for the diameters in the drawing direction and perpendicular to it.

The dependence of the critical diameters $a_{kc}$ of the microvoids which relax at a specific annealing temperature $T_a$ on $T_a$ can be represented by a straight line in a plot of $1/a_{kc}$ *versus* $T_a$ (*Figure 7*). The size of the microvoids relaxing at a particular temperature is thus inversely proportional to the temperature. This result enables us to determine energetic properties of the microvoids. For this purpose, we will make use of the structural model of microvoids discussed above. It will lead to consistent results as we will show below.

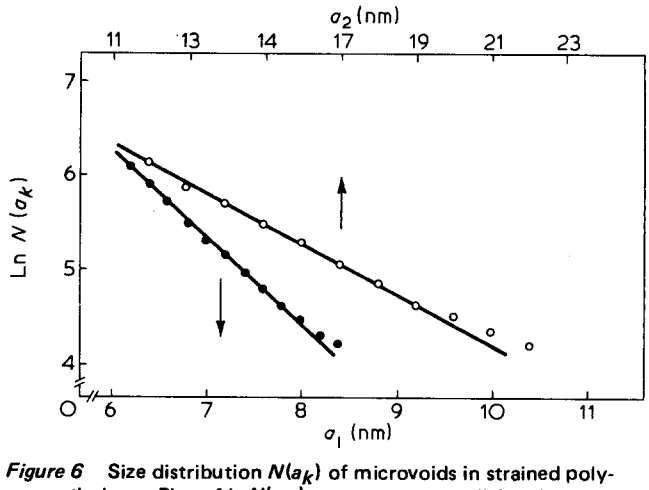


*Figure 6* Size distribution $N(a_K)$ of microvoids in strained polyoxymethylene. Plot of $\ln N(a_K)$ *versus* $a_K$, $a_1$ parallel and $a_2$ perpendicular to the drawing direction

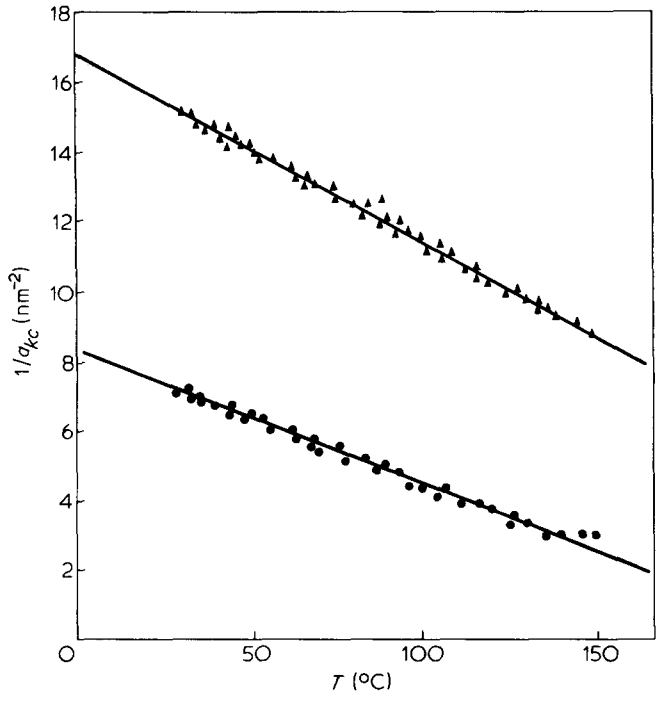


*Figure 7* Plots of $1/a_{1c}$ (▲) and $1/a_{2c}$ (●) (where $a_{kc}$ is the critical size of relaxing microvoids) *versus* temperature $T$

According to this model (equation 3) we have to assume that compressive stresses $\sigma_D$ are exhibited by the microvoids, which are determined by their sizes and the value of the surface free energy. These compressive stresses do not result in the relaxation of the microvoids at room temperature. Internal stresses $\sigma_i$ in the matrix surrounding the microvoids must thus balance the stresses due to the microvoids. Microvoids become able to relax only if these internal stresses $\sigma_i$ become weak. This may be induced by raising the temperature. The relaxation of microvoids involves large scale translational motions of the material surrounding them e.g. translational motions of mosaic blocks. We therefore relate the stress necessary for this motion with the stress at which large scale motions occur at a macroscopical scale, i.e. to the yield stress:

$$\sigma_i = f\sigma_a \tag{14}$$

The parameter $f$ can be considered to represent the stress concentration due to an inhomogeneous stress distribution: it is unity if the local stress surrounding of the microvoids agrees with the nominal stress.

Relaxation of the microvoids becomes possible if the local stress $\sigma_i$ becomes smaller than the compressive stress $\sigma_D$ of the microvoids, due to an increase of the temperature. Combining the expressions representing the temperature dependence of the yield stress (6) and the size dependence of the compressive stress of the microvoids (3) we obtain the following expressions:

$$\sigma_D = \sigma_i = f\sigma_a \rightarrow \frac{A\sigma_l}{a} = f(\sigma_{ao} - jT) \tag{15}$$

which describes the dependence of the diameters of relaxing microvoids ($d \rightarrow a$) on the temperature and relates macroscopical mechanical properties to properties of microvoids.

For a particular geometry of the microvoids (rotational ellipsoids, approximately represented by discs with diameter $\bar{a}_2$ and height $\bar{a}_1$) and for a particular value of $f$ (we assume $f = 1$), equation (15) can be used to calculate the value of the surface free energy. The value obtained is 130 erg cm$^{-2}$ for sample A. The value is of the same order of magnitude as the values obtained from studies on crystallization kinetics and contact angles. This indicates that microvoid formation does not involve extensive chain breakage or plastic flow. These processes may increase the effective value of the surface free energy by several orders of magnitude above the value determined by secondary bonding between the molecules[1,21].

A sample which contains microvoids is unstable thermodynamically. It is not able to approach the equilibrium (microvoid-free) state for kinetic reasons. The same occurs in the glassy state. An increase in temperature leads, in both cases, to a relaxation towards the equilibrium state (enthalpy relaxation for glasses). Excess free energy or excess enthalpy, respectively, are released.

The total excess free energy $G_D$ stored in microvoids is given by:

$$G_D = N_{total}\,\bar{O}\,\sigma_l \tag{16}$$

where $\bar{O}$ is the average surface of a microvoid. The value of this free energy increases exponentially with increasing strain. A plot of $\ln G_D$ *versus* $\epsilon_f$ gives a straight line[17,18]. The exponential dependence is attributed to an exponential increase in the number of microvoids with increasing strain.

## DISCUSSION

### *Correlation between macroscopical mechanical properties and defect properties*

*Figure 8* represents the correlation between the energy stored in defects *versus* the energy stored mechanically in strained samples. A 45-degree line characterizes a one-to-one relation. The experimental data, obtained for sample A, are close to this line. This shows that the energy which was absorbed during a stress–strain experiment, not dissipated to heat, has been used entirely to create microvoids. The energy is stored in the surface of these microvoids.

These results also show that, actually, $f$ must be 1, i.e. an homogeneous stress distribution must exist throughout the material – the experimental data all lie below the 45 degree line; they should lie above this line for $f > 1$.

On the basis of the results described above, we will attempt to describe the relation between the stress–strain behaviour of polyoxymethylene and the formation of microholes.

The stress necessary to obtain specific strain will increase approximately in a linear fashion with increasing strain for small strains. *No microvoids are formed in this range.* This behaviour prevails up to a critical value of the stress $\sigma_c$ (true yield stress) which depends on the strain rate and the morphological structure of the material. Defects are created at this particular value of the stress. The formation of each microvoid results in an incremental increase of the strain at constant stress. The stress will be independent of the strain as long as this process takes place. It occurs homogeneously throughout the sample, and without neck formation. The yielding and the value of the yield stress is thus determined by the defect formation mechanism.

The stress–strain curve of a previously strained sample, which already contains defects, differs strongly from that of the unstrained samples, since the concentration of the

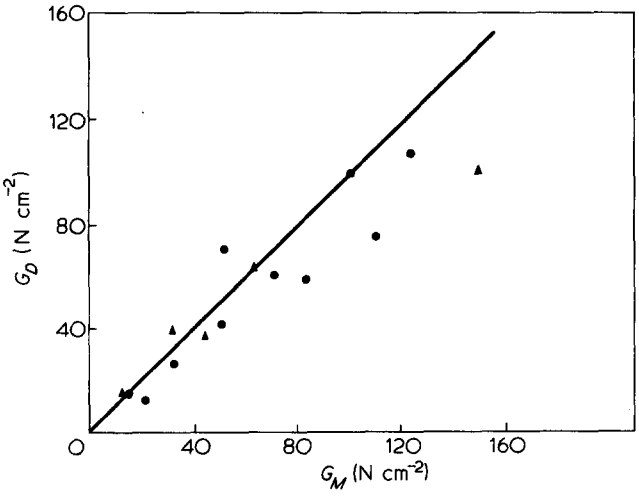


*Figure 8* Plot of mechanically stored energy $G_M$ *versus* energy in microvoids $G_D$ for two series of equally prepared samples (●,▲)

microvoids is sufficient to obtain a specific strain without the formation of new microvoids. Thus, the energy necessary to attain a specific strain is lower than the corresponding value for the unstrained sample. The same is true for the stress. If the strain becomes larger than the value which corresponds to the concentration of defects present, one expects that the stress approaches the yield stress. This is in agreement with the experimentally observed behaviour.

The annealing of the samples resulted in a relaxation of particular microvoids, shown by small angle X-ray diffraction. Thus, the stress–strain curve of the annealed samples must approach the constant yield stress at a lower strain than the unannealed samples, in agreement with the experimental observations.

Our discussion emphasizes the strong correlation between the stress–strain behaviour and the formation of defects for polyoxymethylene.

The experimental data for sample B lie below the 45 degree line in *Figure 8*. The value of the surface free energy for these samples must be lower than those of sample A. It cannot be determined by the annealing procedure described above, since this leads to structural changes for sample B. If we choose a value of $\sigma_l$, which is much lower than the corresponding value for sample A, namely $\approx$48 erg cm$^{-2}$, we again discover a good correlation between defect properties and mechanical properties. This lower value can be attributed to a lower degree of crystallinity: the basic deformation mechanism is apparently unchanged.

## REFERENCES


1 Andrews, E. H. in 'Fracture in Polymers', Oliver and Boyd, London, 1968
2 Ward, I. M. in 'Mechanical Properties of Solid Polymers', Wiley-Interscience, London, 1971
3 Retting, W. *Eur. Polym. J.* 1970, **6**, 853
4 Grabec, I. and Peterlin, A. *J. Polym. Sci., Polym. Phys. Edn.* 1978, **14**, 651
5 Peterlin, A. *Polym. Prepr.* 1977, **18**, 94
6 Olf, H. G. and Peterlin, A. *J. Polym. Sci., Polym. Phys. Edn.* 1974, **12**, 2209
7 Kambour, R. P. *J. Polym. Sci., Macromol. Rev.* 1973, **7**, 1
8 Hull, D. in 'Deformation and Fracture of High Polymers', Plenum Press, 1974
9 Becht, J., De Vries, K. L. and Kausch, H. H. *Eur. Polym. J.* 1971, **7**, 105
10 Johnsen, U. and Klinkenberg, D. *Kolloid Z. Z. Polym.* 1973, **251**, 843
11 Klinkenberg, D. *Progr. Colloid Polym. Sci.* in press
12 Zhurkov, S. N. and Korsukov, V. E. *J. Polym. Sci., Polym. Phys. Edn.* 1974, **12**, 385
13 Kuksenko, V. A., Ryskin, V. S., Betekhtin, V. I. and Slutsker, A. I. *Int. J. Fract.* 1975, **11**, 829
14 Zhurkov, S. N. and Kuksenko, V. S. *Int. J. Fract.* 1975, **11**, 629
15 Zhurkov, S. N., Kuksenko, V. S. and Slutsker, A. I. in 'Fracture *Proceedings of the 2nd International Conference on Fracture,* Brighton, UK, 1969, 531
16 Regel, V. R., Leksovski, A. M. and Sakiev, S. N. *Int. J. Fract.* 1975, **11**, 841
17 Wendorff, J. H. *Angew. Makromol. Chem.* 1978, **74**, 203
18 Wendorff, J. H. *Prog. Colloid Polym. Sci.* 1979, **66**, 135
19 Debye, P. *Z. Phys.* 1959, **156**, 256
20 Gunier, A. in 'Small angle scattering of X-rays', Wiley, New York, 1955
21 Andrews, E. H. and Reed, P. E. *Adv. Polym. Sci.* 1978, **27**, 1
22 Kausch, H. H. in 'Polymer Fracture', Springer-Verlag, Berlin, 1978